



Linear response for pseudo-Hermitian Hamiltonian systems: Application to \mathcal{PT} -symmetric qubitsL. Tetling , M. V. Fistul, and Ilya M. Eremin *Institut für Theoretische Physik III, Ruhr-Universität Bochum, Bochum 44801, Germany*

(Received 17 June 2022; accepted 22 September 2022; published 19 October 2022)

Motivated by recent advances in modeling *pseudo-Hermitian Hamiltonian* (pHH) systems using superconducting qubits, we analyze their quantum dynamics subject to a small time-dependent perturbation. In particular, we develop the linear response theory formulation suitable for application to various pHH systems and compare it to the ones available in the literature. We derive analytical expressions for the generalized temporal quantum-mechanical correlation function $C(t)$ and the time-dependent dynamic susceptibility $\chi(t) \propto \text{Im} C(t)$. We apply our results to two \mathcal{PT} -symmetric non-Hermitian quantum systems: a single qubit and two unbiased/biased qubits coupled by the exchange interaction. For both systems, we obtain the eigenvalues and eigenfunctions of the Hamiltonian and identify \mathcal{PT} -symmetry unbroken and broken quantum phases and quantum phase transitions between them. The temporal oscillations of the dynamic susceptibility of the qubits polarization (z projection of the total spin), $\chi(t)$, relate to ac -induced transitions between different eigenstates and we analyze the dependencies of the oscillation frequency and the amplitude on the gain/loss parameter γ and the interaction strength g . Studying the time dependence of $\chi(t)$, we observe different types of oscillations, i.e., undamped, heavily damped, and amplified ones, related to the transitions between eigenstates with broken (unbroken) \mathcal{PT} symmetry. These predictions can be verified in the microwave transmission experiments allowing controlled simulation of the pHH systems.

DOI: [10.1103/PhysRevB.106.134511](https://doi.org/10.1103/PhysRevB.106.134511)**I. INTRODUCTION**

Coherent quantum mechanics on the macroscopic scale is well established for isolated systems, and many fascinating effects like quantum beats and microwave-induced Rabi oscillations [1], precise manipulation of quantum bits (qubits) [2], maximally entangled Bell and Greenberger-Horne-Zeilinger states [3–5], collective quantum phases and phase transitions [6,7], and nonequilibrium time crystals [8–10] have been observed in optical, magnetic, semiconducting, and superconducting systems [11]. However, even a weak interaction of the quantum system with an environment results in unavoidable dissipation and decoherence leading to the relaxation of an excited quantum state population or the decay of quantum coherent oscillations on large times.

A rapid development of quantum information technologies has allowed not just to fabricate quantum systems extremely weakly interacting with an environment, which is a necessary condition to observe the coherent quantum dynamics at larger times, but also to realize the opposite effect with a nonequilibrium growth of the population of specially chosen quantum states, i.e., the so-called states with a *gain*. Consequently, a *loss* present in other parts of the system is then completely equalized by an induced gain and, as a result, the system can be described within the parity-time (\mathcal{PT})-symmetric non-Hermitian Hamiltonian, which belongs to the broader class of pseudo-Hermitian Hamiltonians (pHHs) [12]. The dynamics governed by \mathcal{PT} -symmetric non-Hermitian Hamiltonians has been implemented in various one- and two-dimensional photonic lattices [13–15], trapped ions and ultracold atoms [16,17], Bose-Einstein condensate [18], as well as

superconducting [19,20] and nitrogen-vacancies qubits [21]. Here, the parity (P) operator in arrays of interacting spins (qubits) is the direct product of local $\hat{\sigma}_i^x$ operators, while the transformation of $i \rightarrow -i$ determines the time-reversal symmetry.

A theoretical analysis of the systems, whose quantum dynamics is described by an arbitrary non-Hermitian Hamiltonian, started a long time ago [22] but was boosted enormously by the seminal works of Bender and coworkers [23–25]. In particular, they have shown that the \mathcal{PT} -symmetric non-Hermitian Hamiltonian can exhibit a purely real eigenvalues spectrum, identifying the *unbroken* \mathcal{PT} -symmetric quantum phase. At the same time as the gain/loss parameter varies, there is also another regime of the Hamiltonian where the eigenvalues of the \mathcal{PT} -symmetric Hamiltonian become complex conjugate ones, signaling the *broken* \mathcal{PT} -symmetric quantum phase, where the so-called exceptional point (line) determines the quantum phase transition (QPT) between \mathcal{PT} -symmetric preserved and broken quantum phases.

These unique quantum phases and transitions between them have been observed in an overwhelming numbers of experimental studies [13–17,19,20]. More complex and intriguing physical phenomena like flat bands [26], anyonic-parity-time symmetry [27], topological defects [28,29], and topological phases [30–34] have been investigated in \mathcal{PT} -symmetric non-Hermitian Hamiltonian systems. Typically, the dynamics of such systems was experimentally studied through the observation of specific time dependencies of the excited-state population, i.e., the oscillating (\mathcal{PT} -symmetry preserved quantum phase) and decaying (\mathcal{PT} -symmetry broken quantum phases) ones.

At the same time, another powerful method to measure various transitions in Hamiltonian systems [35–38] is the spectroscopic one in which the systems dynamics is probed by applying an external small time-dependent perturbation, usually in the form of the electromagnetic field. For Hermitian systems, the quantitative analysis of this spectroscopic method is based on the well-established Kubo linear response theory [39,40]. Therefore, natural questions arise: What is the linear response of a PT -symmetric non-Hermitian Hamiltonian system to a low intensity external ac electromagnetic field? What are the transitions that can be excited by a weak time-dependent perturbation in non-Hermitian systems? Previously, the question on the linear response was analyzed in various systems such as the non-Hermitian Dirac or Weyl Hamiltonians [41–43], or the one- and two-dimensional Bose-Hubbard model [44,45] assuming non-Hermitian/Hermitian types of perturbation [41,42,44] or complex non-Hermitian dissipation operator [45].

In this paper, we discuss a generic *linear response theory* for PT -symmetric non-Hermitian Hamiltonian systems subject to a small time-dependent Hermitian (physical) perturbation. Considering the PT -symmetry Hamiltonian as a particular class of the pseudo-Hermitian Hamiltonian (pHH) [12,46–48], we provide a straightforward way to obtain the generalized temporal correlation function $C_{aa}(t)$ and the linear response function $\chi_{aa}(t)$ of the physical observable a , keeping in mind that the relevant experimental setup in which the coupling between a non-Hermitian system and an external electromagnetic field occurs through a physical observable, i.e., a Hermitian operator. We apply our generic results to an analytical and numerical study of the quantum dynamics in two specific quantum systems: PT -symmetric single qubit and two interacting qubits. In particular, we obtain the dependence of eigenvalues E_i on crucial parameters of the system, i.e., the gain/loss and the qubits interaction strength, identify various quantum phases and exceptional points (lines), and calculate the generalized temporal correlation function $C(t)$ and the linear response function $\chi(t)$ of the total polarization of qubits. The oscillations of $\chi(t)$ determine ac -induced transitions between various states in PT -symmetric non-Hermitian Hamiltonian systems.

The paper is organized as follows: In Sec. II, we review the main points of the quantitative description of the pHH system dynamics, introduce the pseudometric operator $\hat{\eta}$, and demonstrate a generic procedure how to calculate $\hat{\eta}$. In Sec. III, the dynamics of pHH systems subject to a small time-dependent perturbation is studied, and the generic expressions for the time-dependent response function and the generalized temporal correlation function will be obtained. In next two sections, we calculate analytically and numerically the eigenvalues and eigenfunctions for two PT -symmetric exemplary non-Hermitian quantum systems: a single qubit (Sec. IV) and two coupled qubits with the exchange-type interaction (Sec. V). Analyzing the observed oscillations of the imaginary part of the temporal correlation function of the qubit polarization, $\chi(t)$, the dependencies of ac -induced transitions between different states on the gain/loss parameter γ and the interaction strength g are obtained. Both PT -symmetry unbroken and broken quantum phases are studied. We conclude with Sec. VI.

II. GENERAL DESCRIPTION OF PSEUDO-HERMITIAN HAMILTONIAN SYSTEMS

Following the seminal works [23,25] and keeping in mind the application of the elaborated analysis to particular physical systems, i.e., interacting qubits, we review here a general mathematical description of the pHH quantum dynamics [12,46–48].

Let us consider a system whose dynamics is completely determined by pHH, i.e., the Hamiltonian \hat{H}_s satisfies the following condition:

$$\hat{\eta}\hat{H}_s = \hat{H}_s^\dagger\hat{\eta}, \quad (1)$$

where $\hat{\eta} = \hat{\eta}^\dagger$ is a pseudometric Hermitian operator. Note $\hat{\eta}$ is not uniquely defined and, in general, there are N non-commuting operators $\hat{\eta}$ for an N -dimensional pHH [49,50]. Moreover, the operator $\hat{\eta}$ can also be time dependent [19–21]. The dynamics of such a system is characterized by the time-dependent wave function $\Psi(t)$ satisfying the dynamic (Schrödinger-like) equation:

$$i\hbar\frac{d\Psi(t)}{dt} = \hat{H}_s\Psi(t). \quad (2)$$

As \hat{H}_s does not depend explicitly on time, there are two conserved quantities for a *fixed* pseudometric operator $\hat{\eta}$: the total general norm $\langle\Psi(t)|\hat{\eta}|\Psi(t)\rangle$, which is equal to 1 with the proper normalization of Ψ , and the effective Hamiltonian $\langle\Psi(t)|\hat{\eta}\hat{H}_s|\Psi(t)\rangle$.

Since the arbitrary physical measurement has to result in the observation of real values, we define the quantum-mechanical averaging of the physical observable a [51] as

$$\bar{a}(t) = \langle\Psi(t)|\hat{a}|\Psi(t)\rangle = \langle\Psi(0)|e^{i\hat{H}_s^\dagger t/\hbar}\hat{a}e^{-i\hat{H}_s t/\hbar}|\Psi(0)\rangle. \quad (3)$$

Here, the Hermitian operator \hat{a} associates with the physical observable a , and $\Psi(0)$ is the wave function of the initial state. To use the Heisenberg representation and the corresponding equation of motion, it is convenient to introduce the pseudo-Hermitian operator \hat{A} related to the operator \hat{a} of the physical observable a as

$$\hat{A} = \hat{\eta}^{-1}\hat{a}. \quad (4)$$

Since \hat{a} is the Hermitian operator, one finds that \hat{A} satisfies Eq. (1). Throughout the text, we will now use lowercase for the Hermitian physical observable operators and uppercase for the pseudo-Hermitian ones. For time-dependent operators $\hat{A}(t)$, the standard Heisenberg representation is valid,

$$\hat{A}(t) = e^{i\hat{H}_s^\dagger t/\hbar}\hat{A}e^{-i\hat{H}_s t/\hbar}, \quad (5)$$

and, therefore, Eq. (3) can be rewritten as

$$\bar{a}(t) = \langle\Psi(t)|\hat{a}|\Psi(t)\rangle = \langle\Psi(0)|\hat{\eta}\hat{A}(t)|\Psi(0)\rangle. \quad (6)$$

Note Eqs. (1)–(6) present themselves a complete description of the dynamics of arbitrary systems characterized by a time-independent pHH. However, to proceed further, we need to derive an explicit expression for the pseudometric operator $\hat{\eta}$. Assuming the finite Hilbert space and that the Hamiltonian \hat{H}_s is diagonalizable, one can see that \hat{H}_s has a discrete spectrum E_n and a complete, bounded biorthonormal set of eigenfunctions: $|R_n\rangle$ (right states) and $|L_n\rangle$ (left states), where the

equations $\langle L_m | R_n \rangle = \delta_{mn}$ and $\sum_n |R_n\rangle \langle L_n| = \mathbb{1}$ are satisfied. Here, $|R_n\rangle$ and $|L_n\rangle$ are the eigenfunctions of the Hamiltonians \hat{H}_s and \hat{H}_s^\dagger , accordingly: $\hat{H}_s |R_n\rangle = E_n |R_n\rangle$, $\hat{H}_s^\dagger |L_n\rangle = E_n^* |L_n\rangle$. Notice that the generalization to the degenerate eigenvalues is straightforward. The eigenvalues E_n of \hat{H}_s are either real or emerge in complex conjugated pairs [52].

By making use of the eigenvalues E_n and eigenfunctions $|L_n\rangle$, the pseudometric operator $\hat{\eta}$ is explicitly calculated as

$$\hat{\eta} = \sum_{E_n \in \mathbb{R}} |L_n\rangle \langle L_n| + \sum_{E_{n+} \in \mathbb{C}} (|L_{n+}\rangle \langle L_{n-}| + |L_{n-}\rangle \langle L_{n+}|), \quad (7)$$

where the first sum contains all *real* eigenvalues and the second sum runs over *complex* eigenvalues with a positive imaginary part.

III. LINEAR RESPONSE THEORY FOR PSEUDO-HERMITIAN HAMILTONIAN SYSTEMS

The quantitative description elaborated on in the previous section is a good starting point to derive a general expression for the linear response of a non-Hermitian system subject to an externally applied time-dependent force $f(t)$. In this case, the total time-dependent Hamiltonian is written as

$$\hat{H}_{\text{tot}}(t) = \hat{H}_s + f(t)\hat{b}, \quad (8)$$

where \hat{b} is the Hermitian operator. This Hamiltonian allows one to adequately describe the relevant experimental spectroscopic setups where a studied pseudo-Hermitian system is coupled to the electromagnetic field probe. The time-dependent operator of the observable a satisfies the dynamic equation:

$$i\hbar \frac{d\hat{a}}{dt} = \hat{a}\hat{H}_{\text{tot}} - \hat{H}_{\text{tot}}^\dagger \hat{a} = \hat{a}\hat{H}_s - \hat{H}_s^\dagger \hat{a} + f(t)[\hat{a}(t), \hat{b}]. \quad (9)$$

By making use of the relation Eq. (4) between the operators \hat{a} and \hat{A} , and Eq. (5), the solution of Eq. (9) is obtained in zeroth order of perturbation series over a small function $f(t)$ as

$$\hat{a}_0(t) = \eta \hat{A}(t). \quad (10)$$

Correspondingly, in the first order of perturbation series, we write the solution as

$$\hat{a}_1(t) = -\frac{i}{\hbar} \int_0^t ds f(s) [\hat{a}_0(t-s), \hat{b}] \quad (11)$$

and, defining the response function $\chi_{ab}(t)$ as $\bar{a}_1(t) = \langle \hat{a}_1(t) \rangle = \int_0^t ds \chi_{ab}(t-s) f(s)$, we obtain the response function for a pHH system:

$$\chi_{ab}(t) = -\frac{i}{\hbar} \langle [\hat{\eta} \hat{A}(t), \hat{\eta} \hat{B}(0)] \rangle_0 \Theta(t). \quad (12)$$

Here, the step function $\Theta(t)$ is introduced to establish the causality, and the averaging $\langle \dots \rangle_0$ occurs over the wave function $\Psi(0)$ of the initial state. As $\hat{b} = \hat{a}$, that we will assume for the rest of the paper, the response function $\chi_{aa}(t)$ is obtained as

$$\chi_{aa}(t) = -\frac{i}{\hbar} \langle [\hat{\eta} \hat{A}(t), \hat{\eta} \hat{A}(0)] \rangle_0 \Theta(t), \quad (13)$$

where $\hat{A}(0)$ and $\hat{A}(t)$ are determined by Eqs. (4) and (5), respectively. The dynamic response of a pHH system to an

external time-dependent perturbation can also be characterized by the generalized temporal correlation function $C_{aa}(t)$ written as

$$C_{aa}(t) = \langle \hat{\eta} \hat{A}(t) \hat{\eta} \hat{A}(0) \rangle_0 \quad (14)$$

and $\chi_{aa}(t) = (2/\hbar) \text{Im} C_{aa}(t) \Theta(t)$.

Note that Eq. (13) allows one to obtain interesting generic properties of the linear response of pHH systems. By inserting all possible intermediate states in Eq. (13), for systems with a *PT-symmetry broken ground state* we can write explicitly:

$$\chi(t) = -i\theta(t) \sum_n \langle R_0 | \hat{\eta} \hat{A} | R_n \rangle \langle R_n | \hat{\eta} \hat{A} | R_0 \rangle \times [e^{\frac{i}{\hbar}(E_1 - E_n)t} - e^{\frac{i}{\hbar}(E_n^* - E_0)t}], \quad (15)$$

where the energies E_0 and E_1 pertain to the PT-symmetry broken ground state, i.e., $E_0 = a - ib$ and $E_1 = E_0^*$. Thus, for a single qubit with gain and loss, where n takes the values 0, 1 only, we obtain $\chi(t) = 0$ in the PT-symmetry broken regime. Therefore, a weak ac electromagnetic field *cannot* excite the transitions between the eigenstates with complex conjugate eigenvalues, which is also a physically expected result [41]. Also, for a more complex system where various combinations of PT-symmetry preserved (broken) states can be realized, Eq. (15) demonstrates the presence of damped oscillations provided by the transitions between the PT-symmetry broken state, $n = 0$, and PT-symmetry preserved excited states.

In next two sections, we now present a detailed analysis of the energy spectrum, phase diagrams, and the response function for two exemplary models from the realm of qubits: *PT*-symmetric single unbiased qubit and a *PT*-symmetric array of interacting unbiased/biased qubits. The dynamics of these qubit systems is determined by the *PT*-symmetric non-Hermitian Hamiltonians written in the spin representation as

$$\hat{H}_{\text{SQ}} = \Delta \hat{\sigma}^x + i\gamma \hat{\sigma}^z \quad (16)$$

for a single unbiased qubit and

$$\hat{H}_{\text{QA}} = \sum_{i=1}^M \left[\frac{\Delta}{2} \hat{\sigma}_i^x + \frac{\epsilon}{2} \hat{\sigma}_i^z + (-1)^i i\gamma \hat{\sigma}_i^z \right] + g \sum_{ij} (\hat{\sigma}_i^+ \hat{\sigma}_j^- + \hat{\sigma}_i^- \hat{\sigma}_j^+) \quad (17)$$

for an array of M interacting qubits. In the latter case, the qubits exchange interaction of strength g is assumed. Here, $\hat{\sigma}_i^{x,y,z}$ are the corresponding Pauli matrices, Δ , ϵ , and γ are off-diagonal and diagonal matrix elements and gain/loss parameters of individual qubits, respectively. For the sake of simplicity, we assume that these parameters are identical for all qubits. The two setups are also shown schematically in Fig. 1. Note that for the larger size qubit systems, the numerical diagonalization may require an application of more sophisticated algorithms [53,54].

A weak coupling of the qubit system to a low-dissipative waveguide (shown at the bottom of Fig. 1) allows us to *directly* obtain $\chi(\omega)$, i.e., the Fourier transform of $\chi(t)$, by measuring the singularities of the electromagnetic waves' transmission coefficient [35–38,55,56].

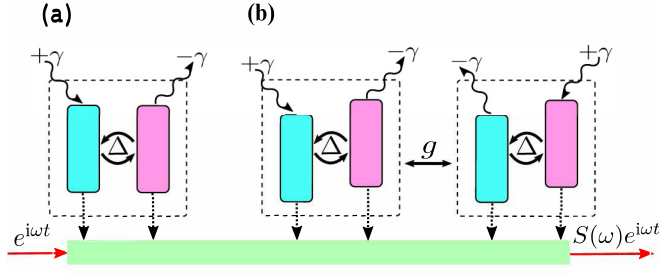


FIG. 1. Schematic representation of PT -symmetric (a) single unbiased qubit and (b) two interacting biased qubits. Here, Δ refers to the off-diagonal coupling between the eigenstates, γ is the process of gain/loss (a staggered gain/loss), and g is an exchange interaction between the qubits. A low-dissipative waveguide couples weakly to qubits and $S(\omega)$ refers to the electromagnetic waves transmission coefficient.

IV. QUANTUM DYNAMICS OF A PT -SYMMETRIC UNBIASED QUBIT

The Hamiltonian Eq. (16) of a single unbiased qubit is invariant under the combined action of operators $\hat{P} = \hat{\sigma}^x$ and $\hat{T} = \mathcal{K}\mathbb{1}$ where time-reversal acts as complex conjugation. The eigenvalues of Eq. (16) can be readily obtained as

$$E_{\pm} = \pm\sqrt{\Delta^2 - \gamma^2} \quad (18)$$

and their dependencies on the parameter γ/Δ are presented in Fig. 2. For $\gamma < \Delta$, the eigenvalues are real and a qubit is in the PT -symmetry preserved (*unbroken*) regime, whereas for

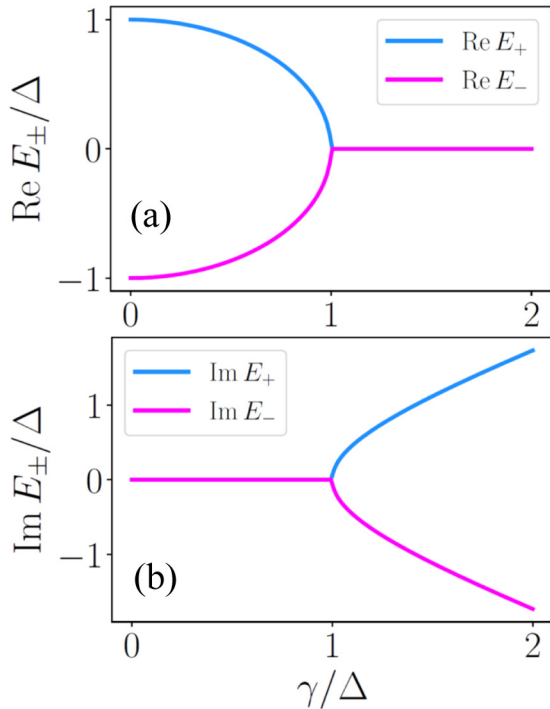


FIG. 2. The dependencies of real (a) and imaginary (b) parts of eigenvalues E_{\pm} on the gain/loss parameter γ/Δ , demonstrating the PT -symmetry preserved and broken quantum phases. The exceptional point is at $\gamma/\Delta = 1$.

$\gamma > \Delta$ the eigenvalues E_{\pm} are conjugated ones with the zero real part and a single qubit in the PT -symmetry broken phase. The condition $\gamma = \Delta$ determines the exceptional point separating the PT -symmetry unbroken and broken quantum phases (see Fig. 2). Next we consider the linear response of the systems in the PT -symmetry preserved and broken regimes.

A. PT -symmetry preserved regime

By making use of the generic results obtained in Sec. II we derive the biorthogonal eigenvectors of the Hamiltonian Eq. (16) as

$$|R_{\pm}\rangle = \frac{\mathcal{N}_{\pm}}{\sqrt{2}} \begin{pmatrix} 1 \\ \frac{\pm E - i\gamma}{\Delta} \end{pmatrix}, \quad |L_{\pm}\rangle = \frac{1}{\sqrt{2}} \begin{pmatrix} 1 \\ \frac{\pm E + i\gamma}{\Delta} \end{pmatrix}, \quad (19)$$

where the normalization coefficients are $\mathcal{N}_{\pm} = \pm \frac{\Delta^2}{E(\pm E - i\gamma)}$ and $E = \sqrt{\Delta^2 - \gamma^2}$. One can verify that $\langle L_m | R_n \rangle = \delta_{mn}$ with $m, n = \pm$ and $\sum_{n=\pm} |R_n\rangle \langle L_n| = \mathbb{1}$. Using Eq. (7), the pseudo-hermitian operator $\hat{\eta}$ is then given by

$$\begin{aligned} \hat{\eta} &= |L_+\rangle \langle L_+| + |L_-\rangle \langle L_-| \\ &= \begin{pmatrix} 1 & -i\frac{\gamma}{\Delta} \\ i\frac{\gamma}{\Delta} & 1 \end{pmatrix}. \end{aligned} \quad (20)$$

Taking into account this expression for $\hat{\eta}$, we proceed with the derivation of the time-dependent qubit polarization (z component of the spin), i.e., $\bar{\sigma}^z(t)$. To make that, we obtain the pseudo-Hermitian operator $\hat{\Sigma}^z$ related to the relevant observable σ^z as

$$\hat{\Sigma}^z = \hat{\eta}^{-1} \sigma^z = \frac{\Delta^2}{\Delta^2 - \gamma^2} \begin{pmatrix} 1 & -i\frac{\gamma}{\Delta} \\ -i\frac{\gamma}{\Delta} & -1 \end{pmatrix}. \quad (21)$$

It is evident that in the limit of $\gamma \rightarrow 0$, the pseudo-Hermitian operator $\hat{\Sigma}^z$ becomes the Hermitian operator $\hat{\sigma}^z$.

Remember that the explicit expression for the time-dependent qubit polarization $\bar{\sigma}^z(t)$ depends on the initial state $\Psi(0)$. Thus, the results become particularly transparent if the initial state is chosen in the basis of z projections of spin, $|\uparrow\rangle = (1 \ 0)^T$. Such an initial state presented in the basis of eigenstates of the Hamiltonian \hat{H}_{SQ} , is given by $|\uparrow\rangle = \frac{1}{\sqrt{2}}(|R_+\rangle + |R_-\rangle)$.

Straightforward but somewhat lengthy calculations [see Eqs. (A3)–(A6) of Appendix A] allow us to derive the nonzero matrix elements of the operator $\hat{\eta} \hat{\Sigma}^z(t)$ as

$$\langle R_- | \hat{\eta} \hat{\Sigma}^z(t) | R_+ \rangle = \frac{\Delta^2}{E(E - i\gamma)} e^{-2iEt/\hbar} \quad (22)$$

and $\langle R_+ | \hat{\eta} \hat{\Sigma}^z(t) | R_- \rangle = \langle R_- | \hat{\eta} \hat{\Sigma}^z(t) | R_+ \rangle^*$. By making use of Eqs. (6) and (22), we obtain in the PT -symmetry preserved regime:

$$\begin{aligned} \bar{\sigma}_{\text{ubr}}^z(t) &= \langle \Psi(0) | \hat{\eta} \hat{\Sigma}^z(t) | \Psi(0) \rangle \\ &= \cos(2Et/\hbar) + \frac{\gamma}{E} \sin(2Et/\hbar). \end{aligned} \quad (23)$$

Not surprisingly, we obtain that the quantum dynamics of a single qubit demonstrates *undamped* oscillations with the frequency $\omega = \sqrt{\Delta^2 - \gamma^2}/\hbar$ in the PT -symmetry preserved regime.

Next we turn to the analysis of the temporal correlation function of the qubit polarization that can be written as

$$C_{\text{ubr}}(t) = \langle \hat{\eta} \hat{\Sigma}^z(t) \hat{\eta} \hat{\Sigma}^z \rangle_0. \quad (24)$$

To study the ac induced transitions, we choose $|R_-\rangle$ as the initial state, that is, the ground state of the Hamiltonian \hat{H}_{SQ} . Using matrix elements of $\hat{\Sigma}^z$ [see Eqs. (A3)–(A6)], we obtain the temporal correlation function $C_{\text{ubr}}(t)$:

$$C_{\text{ubr}}(t) = \frac{\Delta^2}{E^2} \exp(-2iEt/\hbar). \quad (25)$$

The response function of a single qubit in the PT -symmetry preserved regime is determined by the imaginary part of $C_{\text{ubr}}(t)$ as

$$\chi_{\text{ubr}}(t) = \frac{2}{\hbar} \theta(t) \text{Im} C_{\text{ubr}}(t) = 2 \frac{\Delta^2}{E^2} \theta(t) \sin(2Et/\hbar). \quad (26)$$

To conclude this subsection, we note that the Fourier transform of the $\text{Im} C_{\text{ubr}}(t)$, i.e., $\chi_{\text{ubr}}(\omega)$, determines the dynamic susceptibility of the system. In the PT -symmetry preserved regime, the $\chi_{\text{ubr}}(\omega)$ displays a singularity at the frequency $2\sqrt{\Delta^2 - \gamma^2}$. This singularity is related to ac-induced transitions between the pHH eigenstates.

B. PT -symmetry broken regime

In the PT -symmetry broken regime, $\gamma > \Delta$ and the eigenvalues are purely imaginary, i.e., $E_{\pm} = \pm i\tilde{E}$, where $\tilde{E} = \sqrt{\gamma^2 - \Delta^2}$. The eigenvectors are given by

$$|R_{\pm}\rangle = \frac{\mathcal{N}_{\pm}}{\sqrt{2}} \begin{pmatrix} 1 \\ \pm i\tilde{E} - i\gamma \end{pmatrix}, \quad |L_{\pm}\rangle = \frac{1}{\sqrt{2}} \begin{pmatrix} 1 \\ \mp i\tilde{E} + i\gamma \end{pmatrix}, \quad (27)$$

where the normalization coefficients are $\mathcal{N}_{\pm} = -\Delta^2/[E(\tilde{E} \mp \gamma)]$. The orthogonality of the eigenstates is $\langle R_n | L_m \rangle = \delta_{n,m}$, where $n, m = \pm$.

In the PT -symmetry broken regime, the pseudometric operator $\hat{\eta} = |L_+\rangle\langle L_-| + |L_-\rangle\langle L_+|$ is still given by Eq. (20), and also the pseudo-Hermitian operator $\hat{\Sigma}^z$ is determined by Eq. (21). By making use of the results from Appendix B [see Eqs. (B1)–(B6)] and choosing the initial state as $|\uparrow\rangle = (|R_+\rangle + |R_-\rangle)/\sqrt{2}$, we obtain the time-dependent qubit polarization in the PT -symmetry broken regime as

$$\begin{aligned} \bar{\sigma}_{\text{br}}^z(t) &= \langle \Psi(0) | \hat{\sigma}^z(t) | \Psi(0) \rangle \\ &= \cosh(2\tilde{E}t/\hbar) + \frac{\gamma}{E} \sinh(2\tilde{E}t/\hbar). \end{aligned} \quad (28)$$

Thus, one can see that in the PT -symmetry broken regime, the oscillations of the qubit polarization are absent and not just damped, which is a consequence of the eigenenergies being purely imaginary.

In the PT -symmetry broken regime, the temporal correlation function of the qubit polarization $C_{\text{br}}(t)$, calculated for the initial state $|R_-\rangle$, contains only the real part:

$$C_{\text{br}}(t) = \frac{\Delta^2}{\tilde{E}^2} \exp(-2\tilde{E}t/\hbar). \quad (29)$$

and therefore, the linear response function $\chi_{\text{br}}(t)$ is zero in the PT -symmetry broken regime in correspondence to the general Eq. (15).

To conclude this subsection, we notice that Eqs. (23) and (28) for the time-dependent qubit polarization in both preserved and broken regimes have been confirmed in experiments with superconducting [19,20] and nitrogen-vacancy [21] qubits, where the quantity $\bar{\sigma}^z(t)/(\langle \Psi(t) | \hat{1} | \Psi(t) \rangle)$ was measured. Thus, our approach could be directly applied there.

V. QUANTUM DYNAMICS OF PT -SYMMETRIC TWO INTERACTING QUBITS

The quantum dynamics of two interacting PT -symmetric qubits, shown in Fig. 1(b), is governed by the Hamiltonian Eq. (17) with $M = 2$. We stress here that in the presence of the exchange-type interaction between the qubits, and opposite signs of the gain/loss parameter for different qubits, i.e., a staggered gain/loss, the PT symmetry of the Hamiltonian Eq. (17) is preserved even in the biased regime, $\epsilon \neq 0$. However, the PT symmetry in the system of interacting qubits with an arbitrary bias ϵ can only be achieved if the total number of qubits is even. Indeed, for an M -qubit configuration, we define parity and time reversal as

$$\hat{P} \hat{\sigma}_j^\alpha \hat{P}^{-1} = \hat{\sigma}_{N+1-j}^\alpha, \quad \hat{T} i \hat{T}^{-1} = -i, \quad (30)$$

and the operator $\hat{P}\hat{T}$ commutes with the pHH Eq. (17). The disorder in qubit parameters will also break the PT symmetry of the Hamiltonian Eq. (17) but some signatures of the symmetry can still be measured even in a system that inherently breaks PT symmetry [19].

Our strategy is to numerically calculate the eigenvalues E_i and eigenvectors $|R_i\rangle$ ($|L_i\rangle$) to compute the time-dependent linear response of the total qubit polarization for different values of the system parameters like Δ , ϵ , γ , and g . We identify various unbroken and broken PT -symmetry quantum phases and corresponding QPTs for two distinguishable cases, i.e., unbiased and biased interacting qubits.

A. Two unbiased interacting qubits, $\epsilon = 0$

The quantum dynamics of two interacting unbiased qubits is determined by the pHH written explicitly as

$$\begin{aligned} \hat{H}_{2Q} &= \frac{\Delta}{2} \hat{\sigma}_1^x + \frac{\Delta}{2} \hat{\sigma}_2^x - i\gamma \hat{\sigma}_1^z + i\gamma \hat{\sigma}_2^z \\ &+ g(\hat{\sigma}_1^+ \hat{\sigma}_2^- + \hat{\sigma}_1^- \hat{\sigma}_2^+). \end{aligned} \quad (31)$$

The eigenvalues E_i , where $i = 1, \dots, 4$, of \hat{H}_{2Q} are obtained as solutions of the secular equation $P_0(E) = 0$:

$$P_0(E) = E^4 + (\gamma^2 - \Delta^2 - g^2)E^2 - g\Delta^2E. \quad (32)$$

Observe that independently of the qubit parameters, one of the eigenvalues is always zero, $E = 0$. The other three eigenvalues strongly vary with g and γ . The typical dependencies of eigenvalues E_{1-4} on the strength of the interaction g are shown in Figs. 3(a) and 3(b) for two values of γ : $\gamma = 0$ (the Hermitian quantum regime) and $\gamma/\Delta = 0.2$ (the pseudo-Hermitian quantum regime).

For $\gamma \neq 0$, once the interaction strength $|g|$ overcomes the critical values the two PT -symmetry broken quantum phases [indicated in Fig. 3(b) by shaded areas] are realized. In these quantum phases, some eigenvalues are complex conjugated ones. Moreover, for negative (positive) values of g , the

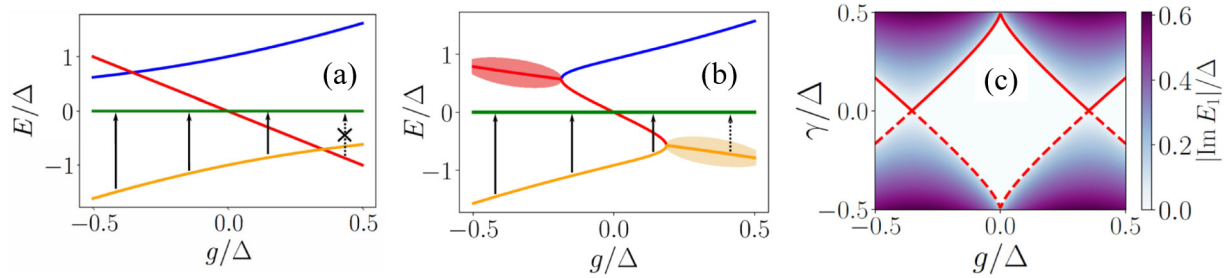


FIG. 3. The eigenvalues of two interacting PT -symmetric unbiased qubits as a function of the interaction strength g/Δ for $\gamma = 0$ (a) and $\gamma/\Delta = 0.2$ (b). The eigenvalues having an imaginary part are shown by shaded area. The arrows indicate the ac-induced transitions between energy levels that can be observed in the linear response $\chi_{2Q}(g; t)$. (c) shows a complete phase diagram demonstrating the presence of preserved (white area) and broken (blue area) PT -symmetry quantum phases. The lines of exceptional points determining the transitions between quantum phases are indicated by red lines.

complex eigenvalues were obtained for the ground (excited) state, and the QPTs between the PT -symmetry preserved and PT -symmetry broken quantum phases can be found, which is similar to the well-known QPTs observed in Hermitian systems of interacting spins [see the regions of $|g| \geq 0.4$ in Fig. 3(a)]. The complete phase diagram $\gamma/\Delta - g/\Delta$ demonstrating the presence of preserved and broken PT -symmetry quantum phases and the lines of exceptional points separating these quantum phases is shown in Fig. 3(c). Comparing Figs. 3(a) and 3(b), one finds that the critical strengths determining the QPTs between broken and unbroken quantum phases shift to lower values as γ increases.

Fixing the gain/loss parameter γ/Δ and choosing the interaction strength g above and below the critical values determining the QPTs between unbroken and broken quantum phases, making use of obtained eigenvalues E_i and eigenfunctions $|R_i\rangle$ ($|L_i\rangle$), we numerically calculate the pseudometric operator $\hat{\eta}_{2Q}$ and the pseudo-Hermitian operator of the total polarization $\hat{\Sigma}_{2Q} = \hat{\eta}_{2Q}^{-1}(\hat{\sigma}_1^z + \hat{\sigma}_2^z)$. In our analysis, we use the minimum energy state of the Hamiltonian Eq. (31) for the initial state $\Psi(0)$. Using further the general results Eqs. (13) and (14), we compute the linear response of the total qubit polarization for two interacting qubits $\chi_{2Q}(g; t)$. In Fig. 4, we show the time dependencies of $\chi_{2Q}(g; t)$ for several particular values of the interaction strength g .

Comparing the left and the right panels of Fig. 4, we register some interesting features of the linear response in the pHH system. For example, in the presence of the PT -symmetric gain/loss γ , the linear response $\chi_{2Q}(t)$ of a PT -symmetry unbroken quantum phase demonstrates undamped quantum oscillations [see Figs. 4(d) and 4(f)]. These oscillations are fingerprints of ac-induced transitions between the ground and excited states indicated by solid arrows in Figs. 3(a) and 3(b). The frequencies of such oscillations decrease substantially with respect to the Hermitian case [compare Figs. 4(c) and 4(e) with Figs. 4(d) and 4(f)]. Notice here that the undamped oscillations are also present for negative values of $g < g_{cr}^{(-)}$ in the PT -symmetry broken quantum phase [see Fig. 4(b)] in which the transitions to the eigenstates with complex conjugated eigenvalues are forbidden. A most spectacular difference between the Hermitian and PT -symmetric non-Hermitian two interacting qubit system is obtained for large positive values of $g > g_{cr}^{(+)}$, e.g., for $g = 0.42$. Indeed, if for $\gamma = 0$ all transitions

are completely forbidden [see Fig. 4(g)], the linear response of the PT -symmetry broken phase shows highly damped oscillations [see Fig. 4(h)]. These oscillations correspond to the ac-induced transition indicated by the dashed arrow in Fig. 3(b). Notice here that the presence of such highly damped oscillations is the direct consequence of Eq. (15).

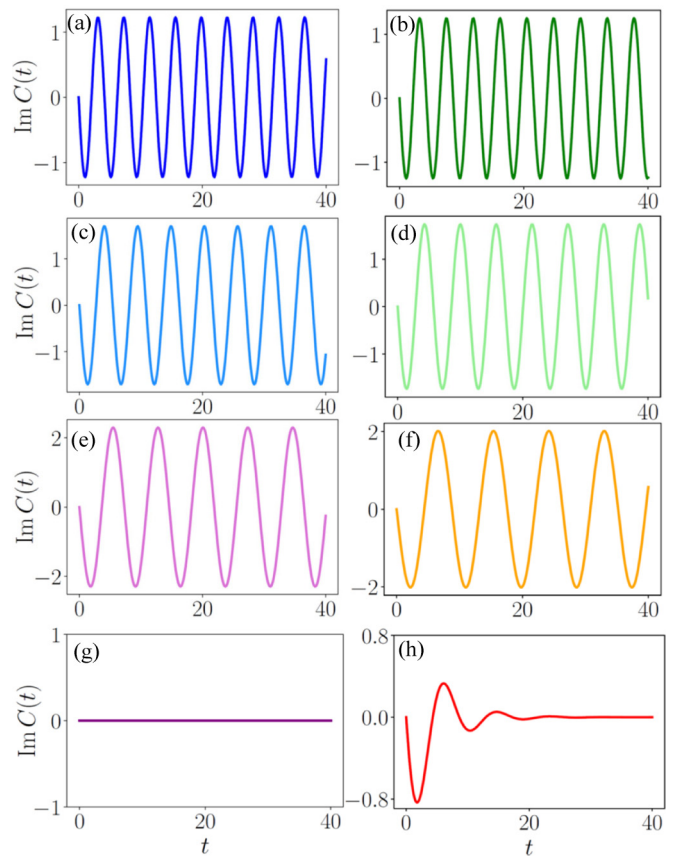


FIG. 4. Time-dependent linear response $\chi_{2Q}(t)$ of the total polarization of two interacting unbiased qubits ($\epsilon = 0$) for two different values of the gain/loss parameter γ , i.e., $\gamma = 0$ (left panels) and $\gamma/\Delta = 0.2$ (right panels). The interaction strength g was chosen as $g/\Delta = -0.42$ (a), (b); $g/\Delta = -0.15$ (c), (d); $g/\Delta = 0.15$ (e), (f); $g/\Delta = 0.42$ (g), (h).

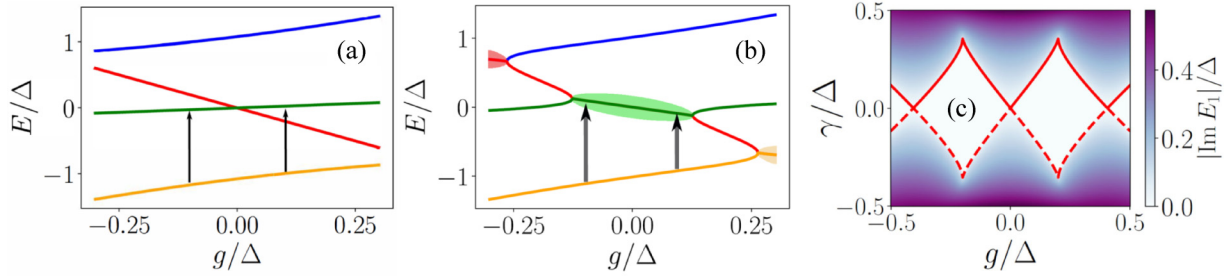


FIG. 5. The eigenvalues of two interacting PT -symmetric qubits with the bias $\epsilon/\delta = 0.2$ as a function of the interaction strength g/Δ for $\gamma/\Delta = 0$ (a) and $\gamma/\Delta = 0.2$ (b). The eigenvalues having an imaginary part are shown by shaded area. (c) shows the complete phase diagram demonstrating the presence of unbroken (white area) and broken (blue area) PT -symmetry quantum phases. The exceptional points determining the transitions between quantum phases are indicated by red lines.

B. Two biased interacting qubits, $\epsilon \neq 0$

The quantum dynamics of two interacting qubits with an arbitrary bias ϵ is determined by the pHH Eq. (17) with $M = 2$. The eigenvalues E_i , where $i = 1, \dots, 4$, of Eq. (17) are obtained as a solution of the secular equation $P_\epsilon(E) = 0$ with

$$P_\epsilon(E) = E^4 + (\gamma^2 - \Delta^2 - g^2 - \epsilon^2)E^2 - g\Delta^2 E + \epsilon^2(g^2 - \gamma^2). \quad (33)$$

The typical dependencies of eigenvalues E_i on the strength of interaction g for biased qubits are shown in Figs. 5(a) and 5(b) for $\gamma = 0$ and $\gamma/\Delta = 0.2$, respectively. Similar to the case of unbiased qubits, the two PT -symmetry broken quantum phases occur for large positive (negative) values of g . However, in the presence of a bias, $\epsilon \neq 0$ and for low values of interaction strength g we obtain an additional PT -symmetry broken quantum phase [see Fig. 5(b), green shaded area]. The complete phase diagram $\gamma/\Delta - g/\Delta$ for biased interacting qubits is presented in Fig. 5(c).

Fixing the interaction strength $g = \pm 0.1$ in the region where such a specific PT -symmetry broken phase can be observed, we compute the dynamic susceptibility of two biased interacting qubits, $\chi_{2Q}(t)$. In Fig. 6, the $\chi_{2Q}(t)$ is presented for two values of γ : $\gamma = 0$ and $\gamma/\Delta = 0.2$. If in the Hermitian

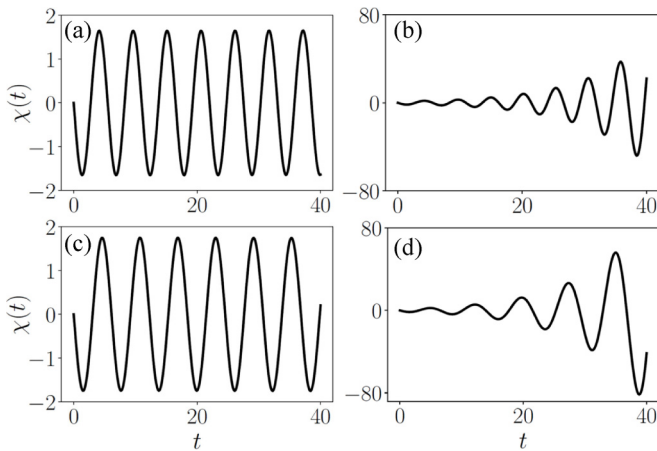


FIG. 6. Time-dependent linear response of the total polarization of two interacting qubits biased at $\epsilon/\Delta = 0.2$ for different values of $\gamma = 0$ (a), (c) and $\gamma/\Delta = 0.2$ (b), (d). The interaction strength g was chosen as $g/\Delta = -0.1$ (a), (b); $g/\Delta = 0.1$ (c), (d).

case ($\gamma = 0$), stable undamped quantum oscillations are found [see Figs. 6(a) and 6(b)], the two PT -symmetric biased interacting qubits demonstrate the *amplified* oscillations [see Figs. 6(c) and 6(d)] related to the ac-induced transitions indicated by arrows in Fig. 5.

VI. CONCLUSION

In conclusion, we have studied in detail the quantum dynamics of qubit systems whose behavior is governed by the PT -symmetric non-Hermitian Hamiltonian. In particular, extending the famous Kubo linear response theory to pHH systems, we derived the general expressions for the temporal quantum-mechanical correlation function $C(t)$ and the time-dependent dynamic susceptibility $\chi(t) \propto \text{Im} C(t)$ [see Eq. (14)], determining the response of pHH systems to a small time-dependent perturbation and identifying various transitions between different states. Their amplitudes, however, are subjects of further normalization by $\langle \Psi(t) | \hat{1} | \Psi(t) \rangle_0$.

Next we have applied the elaborated generic theory to a study of the quantum dynamics of two PT -symmetric quantum systems: a single qubit and two interacting qubits. In such systems, the PT symmetry was introduced in a standard way through the gain and loss exactly compensating each other. For both systems, we observed a variety of PT -symmetry unbroken and broken quantum phases, identifying the QPTs between them as the parameters of gain/loss γ and interaction strength g vary. We derived a complete $\gamma - g$ phase diagram for two PT -symmetric interacting qubits. A peculiar result we obtained is that for two biased PT -symmetric qubits, the excited eigenstates show the PT -symmetry broken behavior even in the absence of the interaction between the qubits.

The quantum dynamics of a PT -symmetric chain of qubits was characterized by the dynamic susceptibility of the total polarization of qubits, $\chi(t)$. The $\chi(t)$ displays oscillations and the corresponding Fourier transform $\chi(\omega)$ shows a number of resonances that are the fingerprints of ac-induced allowed transitions between the eigenstates. Analyzing numerically calculated $\chi(t)$, we identify various transitions between the ground state and excited states for two PT -symmetric interacting qubits [indicated arrows in Figs. 3(b) and 5(b)].

The dynamic susceptibility of the total qubit polarization demonstrates a few generic and interesting features. In particular, for the PT -symmetry preserved phases, the $\chi(t)$

dependence shows undamped quantum oscillations with a frequency that shifts to low values as the parameter γ increases. Moreover, the transition between the PT -symmetry broken ground state and unbroken excited state results in highly damped quantum oscillations in $\chi(t)$ dependence [see Fig. 4(h)]. Furthermore, for two biased interacting qubits, we observe the opposite behavior, i.e., the *amplification* of oscillations in $\chi(t)$ dependence, related to the ac-induced transitions between the PT -symmetry unbroken ground state and broken excited state [see Fig. 6(d)]. We anticipate that these peculiar features of PT -symmetry quantum systems can be observed in spectroscopic experiments with superconducting qubits. Our results can also be straightforwardly generalized to a long chain of qubits.

ACKNOWLEDGMENTS

We thank B. Dora, V. Meden and F. Nogueira for fruitful discussions. We acknowledge financial support through the European Union's Horizon 2020 research and innovation program under Grant Agreement No. 863313 (SUPERGALAX).

APPENDIX A: MATRIX ELEMENTS OF THE PSEUDO-HERMITIAN OPERATORS OF A SINGLE QUBIT: PT -SYMMETRY PRESERVED REGIME

In this Appendix, we provide further details on the calculations of the matrix elements of the pseudo-Hermitian operators for a single qubit system. By making use of the expression Eq. (20), we obtain the operator $\hat{\eta}^{-1}$ as

$$\hat{\eta}^{-1} = \frac{\Delta^2}{E^2} \begin{pmatrix} 1 & i\frac{\gamma}{\Delta} \\ -i\frac{\gamma}{\Delta} & 1 \end{pmatrix}. \quad (\text{A1})$$

With that, the pseudo-Hermitian operator $\hat{\Sigma}^z = \hat{\eta}^{-1}\sigma^z$ can be found as

$$\hat{\Sigma}^z = \frac{\Delta^2}{E^2} \begin{pmatrix} 1 & -i\frac{\gamma}{\Delta} \\ -i\frac{\gamma}{\Delta} & -1 \end{pmatrix}. \quad (\text{A2})$$

In the PT -symmetric unbroken regime, the corresponding matrix elements in the biorthogonal eigenbasis are

$$\langle R_+ | \hat{\Sigma}^z | R_+ \rangle = 0, \quad (\text{A3})$$

$$\langle R_- | \hat{\Sigma}^z | R_- \rangle = 0, \quad (\text{A4})$$

$$\langle R_+ | \hat{\Sigma}^z | R_- \rangle = \frac{\Delta^2}{E(E + i\gamma)}, \quad (\text{A5})$$

$$\langle R_- | \hat{\Sigma}^z | R_+ \rangle = \frac{\Delta^2}{E(E - i\gamma)}. \quad (\text{A6})$$

Using Eqs. (A3)–(A6) and the definition Eq. (5) of the time-dependent operator $\hat{\Sigma}^z(t)$, we obtain the matrix element, which is necessary for the calculation of observable $\bar{\sigma}(t)$ as

$$\begin{aligned} \langle R_- | \hat{\eta} \hat{\Sigma}^z(t) | R_+ \rangle &= \langle R_- | L_- \rangle \langle L_- | R_- \rangle \exp(-iEt/\hbar) \\ &\times \langle R_- | \hat{\Sigma}^z | R_+ \rangle \exp(-iEt/\hbar) = \frac{\Delta^2}{E(E - i\gamma)} \exp(-2iEt/\hbar) \end{aligned} \quad (\text{A7})$$

Here we take into account the normalization condition, i.e., $\langle L_{\pm} | R_{\pm} \rangle = \delta_{\pm, \pm}$. Similarly, we obtain

$$\begin{aligned} \langle R_+ | \hat{\eta} \hat{\Sigma}^z(t) | R_- \rangle &= \langle R_+ | L_+ \rangle \langle L_+ | R_+ \rangle \exp(iEt/\hbar) \\ &\times \langle R_+ | \hat{\Sigma}^z | R_- \rangle \exp(iEt/\hbar) = \frac{\Delta^2}{E(E + i\gamma)} \exp(2iEt/\hbar) \end{aligned} \quad (\text{A8})$$

APPENDIX B: MATRIX ELEMENTS OF THE PSEUDO-HERMITIAN OPERATORS OF A SINGLE QUBIT: PT -SYMMETRY BROKEN REGIME

Here, we provide more details on the matrix elements of the pseudo-Hermitian operator $\hat{\Sigma}^z$ for a single qubit biased in the PT -symmetry broken regime. Taking the eigenstates $|R_{\pm}(L_{\pm})\rangle$ as Eqs. (27) and the explicit expression for the operator $\hat{\Sigma}^z$, i.e., Eq. (21), we obtain the matrix elements of the operator $\hat{\Sigma}^z$ in the biorthogonal eigenbasis as

$$\langle R_+ | \hat{\Sigma}^z | R_+ \rangle = 0, \quad (\text{B1})$$

$$\langle R_- | \hat{\Sigma}^z | R_- \rangle = 0, \quad (\text{B2})$$

$$\langle R_- | \hat{\Sigma}^z | R_+ \rangle = \frac{\Delta^2}{\tilde{E}(\tilde{E} - \gamma)}, \quad (\text{B3})$$

$$\langle R_+ | \hat{\Sigma}^z | R_- \rangle = \frac{\Delta^2}{\tilde{E}(\tilde{E} + \gamma)}. \quad (\text{B4})$$

Similarly to Appendix A, we obtain

$$\begin{aligned} \langle R_- | \hat{\eta} \hat{\Sigma}^z(t) | R_- \rangle &= \langle R_- | L_- \rangle \langle L_- | R_- \rangle \exp(-\tilde{E}t/\hbar) \\ &\times \langle R_+ | \hat{\Sigma}^z | R_- \rangle \exp(-\tilde{E}t/\hbar) = \frac{\Delta^2}{\tilde{E}(\tilde{E} + \gamma)} \exp(-2\tilde{E}t/\hbar), \end{aligned} \quad (\text{B5})$$

and

$$\begin{aligned} \langle R_+ | \hat{\eta} \hat{\Sigma}^z(t) | R_+ \rangle &= \langle R_+ | L_+ \rangle \langle L_+ | R_+ \rangle \exp(Et/\hbar) \\ &\times \langle R_- | \hat{\Sigma}^z | R_+ \rangle \exp(Et/\hbar) = \frac{\Delta^2}{\tilde{E}(\tilde{E} - \gamma)} \exp(2Et/\hbar). \end{aligned} \quad (\text{B6})$$

- [1] M. Kjaergaard, M. E. Schwartz, J. Braumüller, P. Krantz, J. I.-J. Wang, S. Gustavsson, and W. D. Oliver, Superconducting qubits: Current state of play, *Annu. Rev. Condens. Matter Phys.* **11**, 369 (2020).
- [2] F. Arute, K. Arya, R. Babbush, D. Bacon, J. C. Bardin, R. Barends, R. Biswas, S. Boixo, F. G. Brandao, D. A. Buell *et al.*, Quantum supremacy using a programmable superconducting processor, *Nature (London)* **574**, 505 (2019).

- [3] M. Steffen, M. Ansmann, R. C. Bialczak, N. Katz, E. Lucero, R. McDermott, M. Neeley, E. M. Weig, A. N. Cleland, and J. M. Martinis, Measurement of the entanglement of two superconducting qubits via state tomography, *Science* **313**, 1423 (2006).
- [4] C.-P. Yang, Q.-P. Su, S.-B. Zheng, and F. Nori, Entangling superconducting qubits in a multi-cavity system, *New J. Phys.* **18**, 013025 (2016).

- [5] K. Shulga, I. Vakulchyk, Y. Nakamura, S. Flach, and M. Fistul, Time molecules with periodically driven interacting qubits, *Quantum Sci. Technol.* **6**, 035012 (2021).
- [6] A. D. King, J. Carrasquilla, J. Raymond, I. Ozfidan, E. Andriyash, A. Berkley, M. Reis, T. Lanting, R. Harris, F. Altomare *et al.*, Observation of topological phenomena in a programmable lattice of 1,800 qubits, *Nature (London)* **560**, 456 (2018).
- [7] A. D. King, J. Raymond, T. Lanting, S. V. Isakov, M. Mohseni, G. Poulin-Lamarre, S. Ejtemaee, W. Bernoudy, I. Ozfidan, A. Y. Smirnov *et al.*, Scaling advantage over path-integral monte carlo in quantum simulation of geometrically frustrated magnets, *Nat. Commun.* **12**, 1 (2021).
- [8] N. Y. Yao, A. C. Potter, I.-D. Potirniche, and A. Vishwanath, Discrete Time Crystals: Rigidity, Criticality, and Realizations, *Phys. Rev. Lett.* **118**, 030401 (2017).
- [9] S. Choi, J. Choi, R. Landig, G. Kucsko, H. Zhou, J. Isoya, F. Jelezko, S. Onoda, H. Sumiya, V. Khemani *et al.*, Observation of discrete time-crystalline order in a disordered dipolar many-body system, *Nature (London)* **543**, 221 (2017).
- [10] J. Zhang, P. W. Hess, A. Kyprianidis, P. Becker, A. Lee, J. Smith, G. Pagano, I.-D. Potirniche, A. C. Potter, A. Vishwanath *et al.*, Observation of a discrete time crystal, *Nature (London)* **543**, 217 (2017).
- [11] D. Bruss and G. Leuchs, *Quantum Information: From Foundations to Quantum Technology Applications* (John Wiley & Sons, New York, 2019).
- [12] A. Mostafazadeh, Pseudo-Hermiticity versus pt symmetry: The necessary condition for the reality of the spectrum of a non-Hermitian Hamiltonian, *J. Math. Phys.* **43**, 205 (2002).
- [13] C. E. Rüter, K. G. Makris, R. El-Ganainy, D. N. Christodoulides, M. Segev, and D. Kip, Observation of parity-time symmetry in optics, *Nat. Phys.* **6**, 192 (2010).
- [14] R. El-Ganainy, K. G. Makris, M. Khajavikhan, Z. H. Musslimani, S. Rotter, and D. N. Christodoulides, Non-Hermitian physics and pt symmetry, *Nat. Phys.* **14**, 11 (2018).
- [15] A. Szameit, M. C. Rechtsman, O. Bahat-Treidel, and M. Segev, PT-symmetry in honeycomb photonic lattices, *Phys. Rev. A* **84**, 021806(R) (2011).
- [16] L. Ding, K. Shi, Q. Zhang, D. Shen, X. Zhang, and W. Zhang, Experimental Determination of PT-Symmetric Exceptional Points in a Single Trapped Ion, *Phys. Rev. Lett.* **126**, 083604 (2021).
- [17] J. Li, A. K. Harter, J. Liu, L. de Melo, Y. N. Joglekar, and L. Luo, Observation of parity-time symmetry breaking transitions in a dissipative Floquet system of ultracold atoms, *Nat. Commun.* **10**, 855 (2019).
- [18] H. Cartarius and G. Wunner, Model of a pt-symmetric Bose-Einstein condensate in a δ -function double-well potential, *Phys. Rev. A* **86**, 013612 (2012).
- [19] M. Naghiloo, M. Abbasi, Y. N. Joglekar, and K. Murch, Quantum state tomography across the exceptional point in a single dissipative qubit, *Nat. Phys.* **15**, 1232 (2019).
- [20] S. Dogra, A. A. Melnikov, and G. S. Paraoanu, Quantum simulation of parity-time symmetry breaking with a superconducting quantum processor, *Commun. Phys.* **4**, 1 (2021).
- [21] Y. Wu, W. Liu, J. Geng, X. Song, X. Ye, C.-K. Duan, X. Rong, and J. Du, Observation of parity-time symmetry breaking in a single-spin system, *Science* **364**, 878 (2019).
- [22] G. Dattoli, A. Torre, and R. Mignani, Non-Hermitian evolution of two-level quantum systems, *Phys. Rev. A* **42**, 1467 (1990).
- [23] C. M. Bender and S. Boettcher, Real Spectra in Non-Hermitian Hamiltonians Having pt Symmetry, *Phys. Rev. Lett.* **80**, 5243 (1998).
- [24] C. M. Bender, S. Boettcher, and P. N. Meisinger, PT-symmetric quantum mechanics, *J. Math. Phys.* **40**, 2201 (1999).
- [25] C. M. Bender, Making sense of non-Hermitian Hamiltonians, *Rep. Prog. Phys.* **70**, 947 (2007).
- [26] D. Leykam, S. Flach, and Y. D. Chong, Flat bands in lattices with non-Hermitian coupling, *Phys. Rev. B* **96**, 064305 (2017).
- [27] G. Arwas, S. Gadas, I. Gershenzon, A. Friesem, N. Davidson, and O. Raz, Anyonic-parity-time symmetry in complex-coupled lasers, *Sci. Adv.* **8**, eabm7454 (2022).
- [28] A. Stegmaier, S. Imhof, T. Helbig, T. Hofmann, C. H. Lee, M. Kremer, A. Fritzsche, T. Feichtner, S. Klemmt, S. Höfling *et al.*, Topological Defect Engineering and PT Symmetry in Non-Hermitian Electrical Circuits, *Phys. Rev. Lett.* **126**, 215302 (2021).
- [29] C. Yuce and Z. Oztas, Pt symmetry protected non-Hermitian topological systems, *Sci. Rep.* **8**, 1 (2018).
- [30] T. Liu, Y.-R. Zhang, Q. Ai, Z. Gong, K. Kawabata, M. Ueda, and F. Nori, Second-Order Topological Phases in Non-Hermitian Systems, *Phys. Rev. Lett.* **122**, 076801 (2019).
- [31] A. Ghatak and T. Das, New topological invariants in non-Hermitian systems, *J. Phys.: Condens. Matter* **31**, 263001 (2019).
- [32] C.-Y. Ju, A. Miranowicz, G.-Y. Chen, and F. Nori, Non-Hermitian Hamiltonians and no-go theorems in quantum information, *Phys. Rev. A* **100**, 062118 (2019).
- [33] C. Gneiting, A. Koottandavida, A. V. Rozhkov, and F. Nori, Unraveling the topology of dissipative quantum systems, *Phys. Rev. Res.* **4**, 023036 (2022).
- [34] M. Abbasi, W. Chen, M. Naghiloo, Y. N. Joglekar, and K. W. Murch, Topological Quantum State Control through Exceptional-Point Proximity, *Phys. Rev. Lett.* **128**, 160401 (2022).
- [35] A. Blais, J. Gambetta, A. Wallraff, D. I. Schuster, S. M. Girvin, M. H. Devoret, and R. J. Schoelkopf, Quantum-information processing with circuit quantum electrodynamics, *Phys. Rev. A* **75**, 032329 (2007).
- [36] P. Macha, G. Oelsner, J.-M. Reiner, M. Marthaler, S. André, G. Schön, U. Hübner, H.-G. Meyer, E. Il'ichev, and A. V. Ustinov, Implementation of a quantum metamaterial using superconducting qubits, *Nat. Commun.* **5**, 1 (2014).
- [37] K. Shulga, E. Il'ichev, M. V. Fistul, I. Besedin, S. Butz, O. Astafiev, U. Hübner, and A. V. Ustinov, Magnetically induced transparency of a quantum metamaterial composed of twin flux qubits, *Nat. Commun.* **9**, 1 (2018).
- [38] P. Jung, S. Butz, M. Marthaler, M. V. Fistul, J. Leppäkangas, V. P. Koshelets, and A. V. Ustinov, Multistability and switching in a superconducting metamaterial, *Nat. Commun.* **5**, 3730 (2014).
- [39] R. Kubo, Statistical-mechanical theory of irreversible processes. I. General theory and simple applications to magnetic and conduction problems, *J. Phys. Soc. Jpn.* **12**, 570 (1957).
- [40] T. Dittrich, P. Hänggi, G.-L. Ingold, B. Kramer, G. Schön, and W. Zwerger, *Quantum Transport and Dissipation* (WILEY VCH, New York, 1998), Vol. 3.

- [41] D. Sticlet, B. Dóra, and C. P. Moca, Kubo Formula for Non-Hermitian Systems and Tachyon Optical Conductivity, *Phys. Rev. Lett.* **128**, 016802 (2022).
- [42] R. Z. Kiss, D. Sticlet, C. P. Moca, and B. Dóra, Non-Hermitian off-diagonal magnetic response of Dirac fermions, *Phys. Rev. B* **106**, 165411 (2022).
- [43] K. Li and Y. Xu, Non-Hermitian Absorption Spectroscopy, *Phys. Rev. Lett.* **129**, 093001 (2022).
- [44] K. T. Geier and P. Hauke, From non-Hermitian linear response to dynamical correlations and fluctuation-dissipation relations in quantum many-body systems, *PRX Quantum* **3**, 030308 (2022).
- [45] L. Pan, X. Chen, Y. Chen, and H. Zhai, Non-Hermitian linear response theory, *Nat. Phys.* **16**, 767 (2020).
- [46] A. Mostafazadeh, Pseudo-Hermiticity versus PT-symmetry. II. A complete characterization of non-Hermitian Hamiltonians with a real spectrum, *J. Math. Phys.* **43**, 2814 (2002).
- [47] A. Mostafazadeh, Pseudo-Hermiticity versus pT-symmetry III: Equivalence of pseudo-Hermiticity and the presence of antilinear symmetries, *J. Math. Phys.* **43**, 3944 (2002).
- [48] A. Mostafazadeh, Time-dependent pseudo-Hermitian Hamiltonians and a hidden geometric aspect of quantum mechanics, *Entropy* **22**, 471 (2020).
- [49] Z. Bian, L. Xiao, K. Wang, X. Zhan, F. A. Onanga, F. Ruzicka, W. Yi, Y. N. Joglekar, and P. Xue, Conserved quantities in parity-time symmetric systems, *Phys. Rev. Res.* **2**, 022039(R) (2020).
- [50] K. S. Agarwal, J. Muldoon, and Y. N. Joglekar, Conserved quantities in nonHermitian systems via vectorization method, *Acta Polytech.* **62**, 1 (2022).
- [51] Notice here, that in contrast to the PT-symmetric non-Hermitian optical systems the measured quantities in PT-symmetric non-Hermitian qubits systems are $\bar{a}(t)/(\langle\Psi(t)|\hat{\mathbb{I}}|\Psi(t)\rangle)$ but not $\bar{a}(t)$. See also a short comment at the end of Sec. IV.
- [52] A. Mostafazadeh, Pseudo-Hermitian representation of quantum mechanics, *Int. J. Geom. Meth. Mod. Phys.* **7**, 1191 (2010).
- [53] J. Noble, M. Lubasch, and U. Jentschura, Generalized householder transformations for the complex symmetric eigenvalue problem, *Eur. Phys. J. Plus* **128**, 93 (2013).
- [54] J. Noble, M. Lubasch, J. Stevens, and U. Jentschura, Diagonalization of complex symmetric matrices: Generalized householder reflections, iterative deflation and implicit shifts, *Comput. Phys. Commun.* **221**, 304 (2017).
- [55] M. V. Fistul, O. Neyenhuys, A. B. Bocaz, M. Lisitskiy, and I. M. Eremin, Quantum dynamics of disordered arrays of interacting superconducting qubits: Signatures of quantum collective states, *Phys. Rev. B* **105**, 104516 (2022).
- [56] P. Navez, A. Balanov, S. Savel'ev, and A. Zagoskin, Quantum electrodynamics of non-demolition detection of single microwave photon by superconducting qubit array, [arXiv:2205.14490](https://arxiv.org/abs/2205.14490).